www.vbripress.com, www.amlett.com, DOI: 10.5185/amlett.2011.6273 Published online by the VBRI press in 2012

Facile fabrication of uniform silica films with highly luminescent hydrophobic QDs through direct phase transfer

Zhongsen Yang*, Guangjun Zhou

State Key Laboratory of Crystal Materials, Shandong University, Jinan 250100, P. R. China

*Corresponding author. Tel: (+86) 531 88361206; Fax: (+86) 531 88364864; E-mail: zsyang@sdu.edu.cn

Received: 12 June 2011, Revised: 08 Sept 2011 and Accepted: 11 Sept 2011

ABSTRACT

Hydrophobic CdSe/ZnS quantum dots (QDs) were embedded in a transparent functional silica film with thickness of 10-15 μm using a sol-gel method. Namely, the QDs were prepared through an organic synthesis using hexadecylamine as a capping agent. When partially hydrolyzed 3-aminopropyltrimethoxysilane (APS) sol was mixed with a toluene solution of the QDs, the ligand exchange occurred. With subsequent addition of pure H_2O, the QDs were transferred into APS sol accompanied with a phase separation. The APS sol with the QDs was condensed to adjust its' viscosity by the evaporation of solvents at room temperature. After that, functional SiO_2 films with tunable QD concentrations and high photoluminescence (PL) efficiency were fabricated by a spin-coating strategy using the condensed APS sol with the QDs. The absorbance at first absorption peak of the QDs revealed a liner increase against the QD concentrations in these films. The PL peak wavelength and full width at half maximum of PL spectra of the QDs in these films remained unchange compared with their initial values in toluene. The QDs were mono-dispersed in these films according to transmission electron microscopy observation. Due to unique properties, these films are utilizable for further applications in optical and electronic devices.

Keywords: Semiconductor; QDs; luminescence; silica; film.

Zhongsen Yang got his B. Sc. at Jilin University, P.R. China in 1972. He has been working in the State Key Laboratory of Crystal Materials at Shandong University since 1972 as an engineer. His research focused on crystal materials, nanomaterials, magnetic and luminescent materials. Especially, his research is interesting in sol-gel chemistry, combustion synthesis, and photocatalysis.

Introduction

Semiconductor quantum dots (QDs) show unique size-dependent optical properties and are currently of great interest for various prospective applications in photovoltaic devices [**1-4**], optical amplifier media for telecommunication networks [**5**], and for biolabeling [**6, 7**]. The good photostability, high photoluminescence (PL) intensity, and broad emission tunability make these QDs an excellent choice as novel chromophores. To assemble QDs into solid matrices is a critical stage required for their integration with solid-state devices. Several fabrication techniques are widely used to make ultrathin organized and inorganized nanocomposite films including spin casting, Langmuir-Blodgett deposition, and layer-by-layer (LbL) assembly [**8, 9**]. Kotov's [**10**] and Oliveira's [**11**] groups have fabricated multilayered composites with alternating layers of polycation and semiconductor nanoparticles. In another study, Leblanc and co-workers prepared a combined LbL film containing several bilayers of chitosan and CdSe QDs, covered with two bilayers of organophosphorus hydrolase/QDs [**12**].

Luminescence films play an important role in various devices including high resolution devices such as cathode ray tubes, thin fillm electroluminescent panels, and field emission displays. QDs embedded in a film matrix as the protective shell have been reported to provide a high density of light emitting centers by varying the size and concentration of QDs in an ensemble [**13, 14**]. Gallagher et al. [**15**] reported on a luminescent solar concentrator consisting of CdSe/ZnS QDs and polyurethane matrix by casting and curing in polymethylmethacrylate mould. Comparing with polymers, silica is a more excellent matrix, providing good mechanical and optical properties and conferring a high kinetic stability on QDs [**16–18**]. Many researchers have incorporated QDs into transparent silica matrix [**19-21**] and explored their potential applications in QD lasers, wave-guides and high-speed optical switches [**22**]. However, the report on hydrophobic QDs-SiO_2 composite films is rare. It is difficult to directly incorporate hydrophobic QDs in sol-gel SiO_2 films. The QDs have to

be transferred into water phase by ligand exchange, in which the preparation procedure of films becomes complicated. It is still a challenge to retain a high PL efficiency in these films because such complicated procedure resulted in the decrease of PL efficiency [**23**].

Sol–gel approach is a low-temperature alternative to high-temperature chemical vapor deposition synthesis of films. The preparation of sol–gel-derived materials first requires the mixing of the alkoxide, water and a mutual solvent to produce a sol. In the case of silica glasses, the sol–gel process involves the hydrolysis and condensation of a silicon alkoxide precursor to give gels, which can be densified further using a heat treatment program. For the fabrication of thin films the reactions are allowed to proceed for a period of time, the prepolymerization or aging time, between precursor mixing and the coating of samples. This aging time must be less than the gelation time. Following coating, a drying step is carried out to form a hard microporous film. The thickness of silica sol–gel films can be easily varied by selection of the degree of condensation of the primary siloxane oligomers and the withdrawal or spinning rate upon dip- or spin-coating, respectively.

To improve the quality of sol-gel films, a drying step has to be controlled very carefully because the condensation of silica gel resulted in the formation of structure defects. However, this controlling is very difficult. Many other approaches were used to prepare free-defect sol-gel films. For example, the introduction of organic or inorganic doping species to silica sol for the rational design of functional coatings enables the direct tailoring of their properties [**23, 24**]. Functional silane agents are good candidates for such purpose. 3-aminopropyltrimethoxysilane (APS) reveals different hydrolysis and condensation properties compared with tetra orthosilicate (TEOS) which was usually used to prepare sol-gel silica films. We found out a transparent and homogeneous film can be easily created by using APS sol because of a small shrinkage after drying.

In this paper, highly luminescent films with hydrophobic CdSe/ZnS QDs were fabricated by using a sol-gel process including the phase transfer of the QDs by partially hydrolyzed APS to replace hexadecylamine (HDA), the evaporation of the solvents in APS sol to adjust the viscocity of the sol, and the fabrication of films by spin-coating. These films exhibited a high PL efficiency of 20% and tunable QD concentrations.

Experimental

Chemicals

All chemicals were of analytical purity or of the highest purity available. These chemicals were purchased from Sigma Aldrich. Trioctylphosphine (TOP) was additionally purified by distillation.

CdSe/ZnS QDs Synthesis

CdSe core synthesis was based on the methods of Talapin et al. [**25**] and ZnS shell synthesis was based on the method of Ying's group [**26**]. CdSe core was synthesized using cadmium oxide as a precursor and a mixture of trioctylphosphine oxide (TOPO) and HDA as coordinating solvents. In a typical synthesis, CdO (0.50 mmol) and stearic acid (3.12 mmol) were heated to 190-210 °C under an argon atmosphere until a clear, colorless solution was obtained. At this temperature TOPO (7.21 mmol) and HDA (5.75 mmol) were added to the reaction mixture, and the temperature was further increased to 310 °C. Then the heating was stopped, and a solution of Se (0.50 mmol) in 4 mL of TOP was quickly injected into the reaction volume while rapidly stirring, causing an immediate nucleation and growth of nanoparticles.

To synthesize the ZnS shell, zinc acetate dihydrate ($Zn(OAc)_2 \cdot 2H_2O$, 0.4 mmol), 1 g of HDA and 10 mL of trioctylamine were placed in a three-neck round-bottom flask under N_2 flow, and stirred at 260 °C until the Zn salt was completely dissolved. S powder (2 mmol) was dissolved in 4 mL of TOP. The toluene solution of CdSe cores was injected with rapid stirring, followed by the dropwise addition of the TOPS solution. The mixture was kept at 260 °C for another 2.5 h, followed by cooling down to room temperature. The products were precipitated, washed three times with methanol, and re-dispersed in 20 mL of toluene.

Phase transfer of CdSe/ZnS QDs

A precursor APS sol was prepared by mixing APS with ethanol and H_2O. Typically, the molar ratio of ethanol/H_2O/APS is 30/1.5/1. The mixture was stirring for 15 to 24 h and then heat-treated at 50-70 °C to evaporate the ethanol. The toluene solution of CdSe/ZnS QDs (01-2 mL) was mixed with the precursor APS sol of 0.2-1 mL with stirring for 5-10 min. H_2O of 0.1-0.5 mL was added to the mixture with stirring for 10 min. Finally, the hydrophobic QDs were transferred into APS sol accompanied with a phase separation. Toluene was remained on the upper part. The APS sol with the QDs was extracted and centrifuged at 4000 rpm for 2 min for purification.

Film preparation

APS sol with CdSe/ZnS QDs was kept in a beaker at room temperature for 12-24 h under atmospheric conditions. This made the viscosity of the sol 1200-1500 mPa·s. Slide glass substrates were immersed in a fresh aqueous solution of acid ((v/v) 1:3, 30% H_2O_2/98% H_2SO_4) until gas evolution ceased. After being rinsed with copious amounts of water and dried, the surface-treated substrates were spin-coated (900 rpm for 30 s). The central part of the substrates (20 × 20 mm) was cut to obtain transparent functional SiO_2 films. The measurement indicates these films have a uniform thickness (10-15 μm).

Characteristics

Transmission electron microscopy (TEM) observations were carried out using JEM 2100 (JEOL Ltd.) electron microscope with a link energy dispersive X-ray (EDX) analysis system. For the preparation of a TEM specimen, Cu grid was dipped in condensed APS sol with CdSe/ZnS QDs and then taken out quickly to avoid the thickness of film too thick. The absorption and PL spectra were taken using conventional spectrometers (Hitachi U-4100 and F-4600). The PL efficiencies of CdSe/ZnS QDs in functional

silica films were estimated in comparison with a standard rhodamine 6G solution having a similar optical path length and optical density [**27, 28**]. The PL lifetimes were measured using a time-correlated single-photon-counting spectrofluorometer system (FluoroCube-3000U, Horiba). Samples were precipitated by 2-propanol and dried in a vacuum oven for X-ray diffractometer (XRD) characterization with a Bruker D8 diffractometer).

Results and discussion

Fig. 1 shows the absorption and PL spectra of CdSe cores and CdSe/ZnS QDs. A significant red shift of PL peak wavelength (539.0 nm for CdSe cores and 619.5 nm for CdSe/ZnS core-shell QDs) was created with a ZnS shell coating. The observed red shifts both in the PL peak and first absorption peak demonstrated strongly the formation of CdSe/ZnS core-shell QDs. The red shifted absorption and PL spectra of CdSe/ZnS core-shell QDs are ascribed to the growth of ZnS shell on the CdSe core. The red shift upon shell growth is related to a decrease in the kinetic energy of the excited electrons and holes in the QDs due to the spreading of their wave functions into the shell. This red shift also indicates that the QDs are of a core–shell structure.

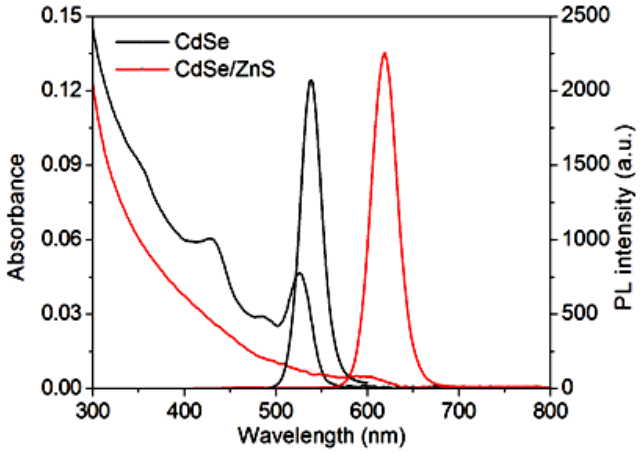

Fig. 1. Absorption and PL spectra of CdSe core and CdSe/ZnS QDs.

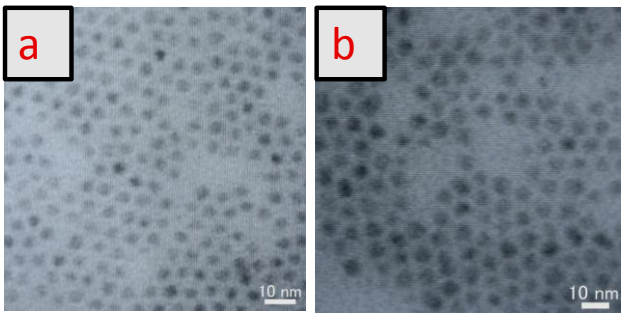

Fig. 2. TEM images of CdSe cores (**a**) and CdSe/ZnS QDs (**b**).

To further confirm the ZnS shell formation on the CdTe cores, **Fig. 2** shows the TEM images of CdSe cores (**a**) and CdSe/ZnS QDs (**d**). The mean size of cores and QDs are 4.0 and 5.1 nm, respectively. This result is same with that estimated by their absorbance at first adsorption peak. These cores and QDs exhibited a narrow size distribution. The XRD patterns of CdSe cores and CdSe/ZnS QDs reveals a cubic zinc-blende structure as shown in **Fig. 3**.

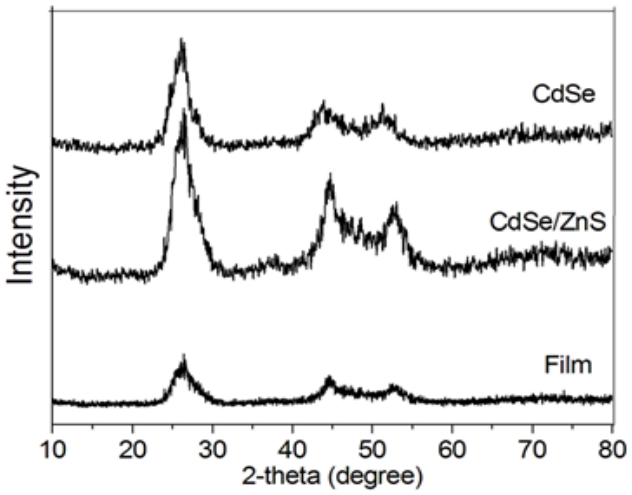

Fig. 3. XRD patterns of CdSe cores, CdSe/ZnS core-shell QDs, and films.

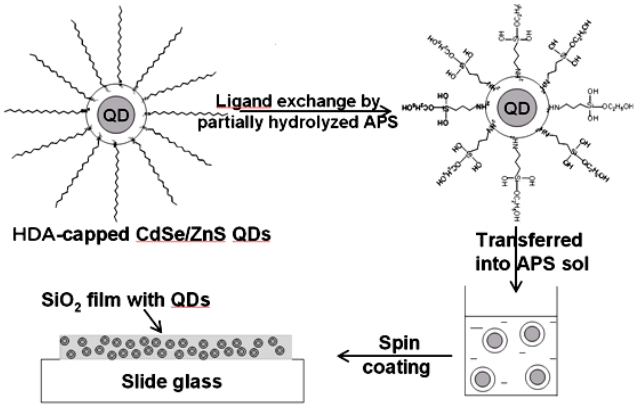

Scheme 1. Preparation procedure of functional SiO_2 film with CdSe/ZnS QDs.

Table 1. Preparation conditions and properties of functional SiO_2 films with CdSe/ZnS QDs

Sample	QD amount added (mL)	Film thickness (μm)	QD concentration (10^{-4} M)	Absorbance at first absorption peak	PL efficiency (%)
1	0.1	11.2	0.09	0.003	19.5
2	0.2	10.3	0.19	0.006	19.8
3	0.3	12.2	0.3	0.011	20.3
4	0.4	12.7	0.34	0.013	19.8
5	0.5	15.0	0.33	0.015	20.0
6	0.7	13.2	0.48	0.019	19.6
7	0.8	11.8	0.65	0.023	19.8
8	0.9	10.6	0.75	0.024	19.3
9	1	11.5	0.84	0.029	18.6
10	1.3	13.9	1.01	0.042	18.2
11	2	14.1	1.39	0.059	17.9

Scheme 1 indicates the preparation procedure of functional SiO_2 films with CdSe/ZnS QDs. The Phase transfer of HAD-capped CdSe/ZnS QDs occurred by using partially hydrolyzed APS because the amino groups in APS have an ability to replace HDA on the QDs. The partially hydrolysis resulted in APS molecules can be dissolved both in toluene and H_2O. The QDs were then transferred into

H_2O phase when pure water was added. This phenomenon is ascribed to partially hydrolyzed APS is highly hydrophilic. The amount of QD solutions was adjusted during preparation for the purpose of tuning the QD concentrations in films. **Table 1** summarizes the preparation conditions and properties of functional SiO_2 films with CdSe/ZnS QDs.

Fig. 4 shows the PL and absorption spectra of functional SiO_2 films with CdSe/ZnS QDs (Sample 9 shown in **Table 1**). The PL peak wavelength and the full width at half maximum (FWHM) of PL spectra of the QDs in films remained unchange compared with those of initial QDs. The PL efficiency of the QDs in films was 20% at a maximum value while the initial value in a toluene solution is 30%. This PL efficiency is still high compared with other QD-polymer and QD-silica films in literature [**5-9**]. The decrease of the PL efficiency of the QDs incorporated in films was ascribed to the change of surrounding environment. Compared with as-prepared QDs, the PL peak wavelength of the film revealed a blue-shift of 0.7 nm while their first absorption peak exhibited a 0.5 nm blue shift. This is ascribed to the ligand exchange after phase transfer.

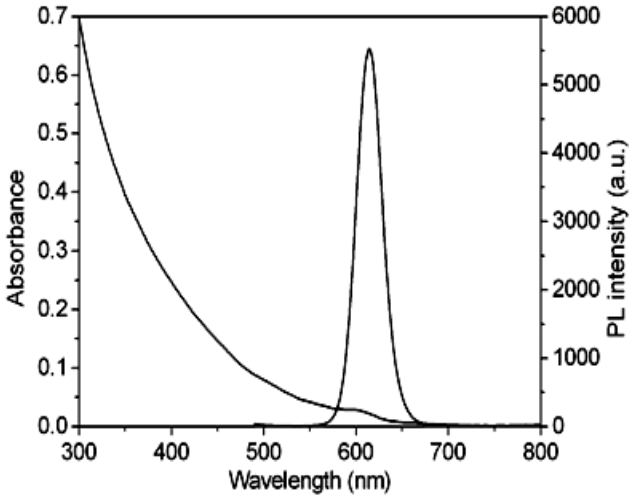

Fig. 4. Absorption and PL spectra of functional SiO_2 films with CdSe/ZnS QDs (Sample 9 shown in **Table 1**)

Ligand exchange reactions have been widely used to modify the surface of QDs to tune QD solubility as well as to provide functionality for further coupling to biomacromolecules [**29**]. For example, water-soluble CdSe/ZnS QDs were created by ligand exchange of TOPO with mercaptocarbonic acid [**30**], which ought to be greatly advantageous due to its simplicity. However, it was found that the PL efficiency of the QDs after the ligand exchange dropped significantly [**31**]. The mechanism of the decrease of PL efficiency has been attributed to ligand exchange between the new ligand and the original capping TOPO molecules, in which surface defects might be generated [**32**]. In our experiment, the ligand exchange between partially hydrolyzed APS and HDA also resulted in the decrease of PL efficiency which was ascribed to the change of surface state of the QDs. Because the ligand exchange occurred in partially hydrolyzed APS sol, the decrease of PL efficiency is not too much.

The concentration of CdSe/ZnS QDs in functional silica films was estimated by using a method reported elsewhere [**33**]. The extinction coefficient per mole of particles (ε) described below will be the values at the first absorption peak position. They were calculated using Lambert-Beer's law.

$$A = \varepsilon CL \qquad (1)$$

In equation 1, A is the absorbance at the peak position of the first exciton absorption peak for a given sample. C is the molar concentration (mol/L) of the QDs of the same sample. L is the path length (cm,) of the radiation beam used for recording the absorption spectrum. In our experiments, L was the thickness of films. ε is the extinction coefficient per mole of nanocrystals (L/mol/cm). The preparation conditions and properties of functional SiO_2 films with CdSe/ZnS QDs are summarized in **Table 1**. As a result, these films revealed relatively high PL efficiencies and high QD concentrations. This phenomenon is associated with the amino group in APS which as folds to avoid the agglomeration of the QDs in these films.

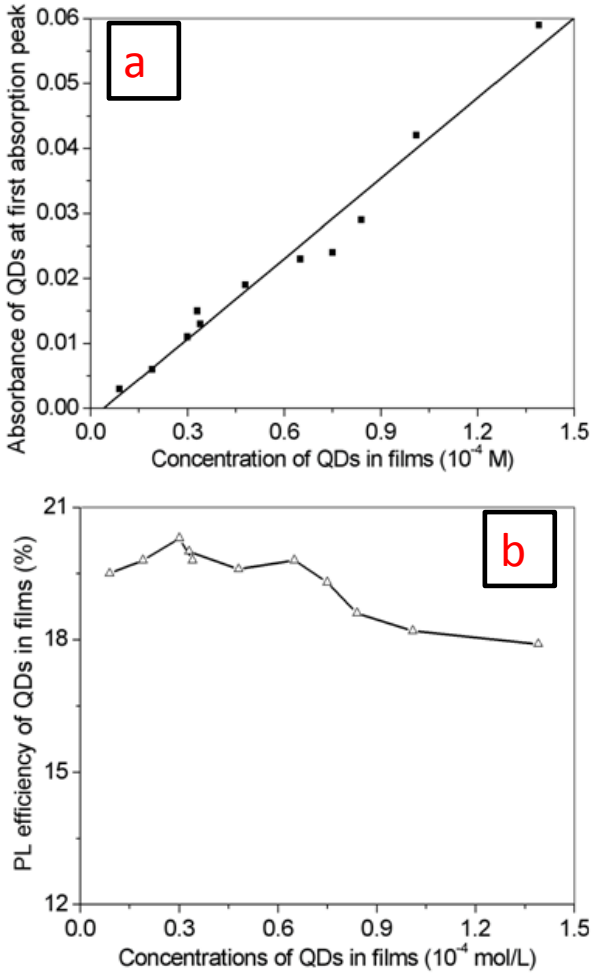

Fig. 5. Absorbance at first absorption peak (**a**) and PL efficiencies (**b**) of QDs versus their concentrations in functional SiO_2 films. The absorbance of the QDs at first absorption peak revealed a liner increase with increasing the QD concentration. The QDs exhibited a PL efficiency of 20 % when the QD concentration is less than 7.5×10^{-5} M.

Fig. 5 shows the absorbance at first absorption peak (a) and PL efficiency (b) of CdSe/ZnS QDs versus the QD concentrations in functional SiO_2 films. The absorbance of the QDs revealed a liner increase with increasing the QD concentration in these films. The QDs exhibited a PL efficiency of 20 % when the concentration of the QDs is less than 7.5×10^{-5} M. The PL efficiencies of the QDs in these films were then decreased because of a concentration effect of PL.

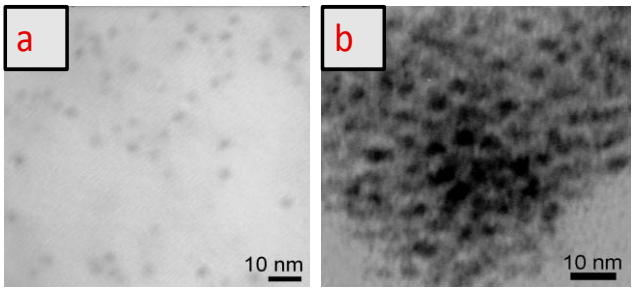

Fig. 6. TEM images of functional SiO_2 films with CdSe/ZnS QDs: (a), Film with QD concentration of 9×10^{-6} M (Sample 1 shown in **Table 1**); (b), Film sample with QD concentration of 1.39×10^{-4} M (Sample 11 shown in **Table 1**).

Table 2. Components B_1 and B_2, time constants τ_1 and, τ_2 of initial CdSe/ZnS QDs and functional SiO_2 film with QDs.

Samples	B_1 (%)	τ_1/ns	B_2 (%)	τ_2/ns	τ/ns	PL efficiency (%)
QDs	45.09	11.43	54.91	22.81	24.6	30
Film	35.26	5.33	64.74	21.67	27.7	20

Fig. 6 shows the TEM images of functional SiO_2 films with CdSe/ZnS QDs: (**a**), the film with QD concentration of 9×10^{-6} M (Sample 1 shown in Table 1); (**b**), the film with QD concentration of 1.39×10^{-4} M (Sample 11 shown in **Table 1**). The QDs were mono-dispersed in films both for Samples 1 and 11. The result indicates the QDs with a mean size of ca. 5.1 nm. This size is almost the same as that derived from the first absorption peak of the QD toluene solution. This indicates that the QDs were dispersed in these films without aggregation. The TEM image also shows a relatively high surface coverage of QDs for Sample 11. The XRD pattern of the films was shown in **Fig. 3**. CdSe/ZnS QDs exhibited in the films exhibited cubic zinc-blende structure. EDX analysis of the films demonstrated Zn component existed in the shell.

Fig. 7 shows the luminescence decay curves (measured at the maximum PL peak, λ_{ex} = 374 nm) of functional SiO_2 films with CdSe/ZnS QDs and initial QDs in toluene. The decay curves can be well fitted to a biexponential model described by $F(t) = A + B_1 exp(-t/\tau_1) + B_2 exp(-t/\tau_2)$, where τ_1 and τ_2 represent the time constants, and B_1 and B_2 represent the amplitudes of the fast and slow components, respectively. The fitted values of the parameters B_1, B_2, τ_1, and τ_2, are shown in **Table 2**. The fast (τ_1), and slow (τ_2) decay of CdSe/ZnS QDs involves recombination of the delocalized carriers and the localized carriers, respectively. The fast component (B_1) of PL decay of the QDs embedded in the film decreased compared with that of initial QDs while the slow component (B_2) increased. As shown in **Table 2**, the lifetime of fast PL decay (τ_1) drastically decreased; however, the lifetime of slow PL decay (τ_2) decreased slightly, which is a characteristic of the localization process of excitons [**34**]. This phenomenon is considered to originate from the surface-related emission of the QDs embedded in the film.

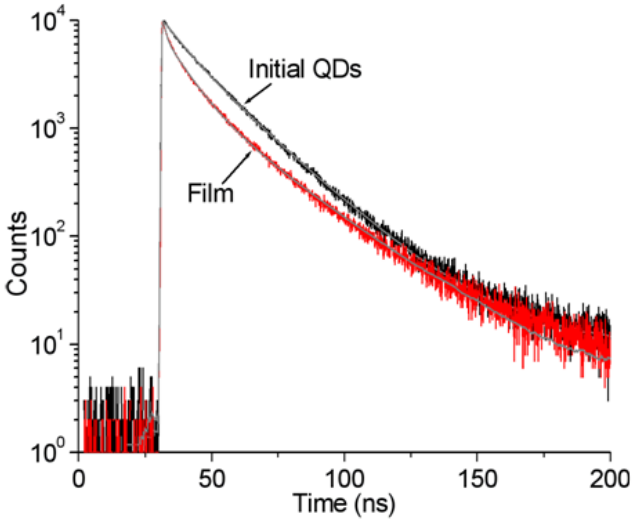

Fig. 7. PL decay curves (measured at maximum emission peak, λ_{ex} = 374 nm) of functional SiO_2 film with CdSe/ZnS QDs and initial QDs in toluene. Reproduced curves for data shown in **Table 2** are plotted as thin gray lines.

Comparing with other QD-polymer films, CdSe/ZnS QDs in functional SiO_2 films exhibited a relatively high PL efficiency at a high QD concentration. One reason is the QDs coated with a partially hydrolyzed APS layer in a mixture of APS sol and a toluene solution of the QDs. The ligand exchange and subsequent phase transfer were carried out within a relatively short reaction time. Condensed APS sol without ethanol also plays an important role for preventing the surface deterioration of the QDs that slowly quenches the PL of the QDs. Such surface reactions were observed in literature [**35**] due to the long preparation cycle. Because the obtained transparent thin films emit strongly, it is fair to expect that they can be used for practical light-emitting devices such as displays, lightening, and the surface layer of a solar cell.

Conclusion

Transparent and highly luminescent functional SiO_2 films with a thickness range of 10-15 μm were fabricated by dispersing hydrophobic CdSe/ZnS QDs. Ligand exchange occurred when HDA-capped CdSe/ZnS QDs were mixed with partially hydrolyzed APS sol. The phase transfer was subsequently created by adding H_2O in the mixture of APS sol and the QDs. The PL efficiency of the QDs in these films was 20 % while their initial value is 30 %. In this incorporation processes, the amino groups in APS plays an important role to avoid the agglomeration of the QDs in films. The PL peaks wavelength and FWHM of PL spectra remained unchange when the QDs embedded in films. The intense PL from the high QD concentration demonstrates

the potential application of these functional QD-SiO_2 films to optical devices.

Acknowledgements
This work was supported in part by projects from National Science Foundation of China (50972081) and Natural Science Foundation of Shandong Province (Y2008F32).

Reference

1. Barnham, K.; Marques, J. L.; Hassard, J.; O'Brien, P. Appl. Phys. Lett. 2000, 76, 1197.
2. Singh, R. P.; Choi, J.-W. Adv. Mat. Lett. 2010, 1, 83. DOI: 10.5185/amlett.2010.4109
3. Rai, R.; Sharma, S. Adv. Mat. Lett. 2010, 1(3), 269. DOI: 10.5185/amlett.2010.7140
4. Varshney, R.; Bhadauria, S.; S.Gaur M. Adv. Mat. Lett. 2010, 1(3), 232-237. DOI: 10.5185/amlett.2010.9155
5. M. T. Harrison, S. V. Kershaw, M. G. Burt, A. L. Rogach, A. Kornowski, A. Eychmuller, H. Weller, Pure Appl. Chem. 72 (2000) 295-307.
6. M. P. Bruchez, M. Moronne, P. Gin, S. Weiss, A. P. Alivisatos, Science 281 (1998) 2013-2016.
7. M. Han, X. Gao, J. Z. Su, S. Nie, Nat. Biotechnol. 19 (2001) 631-635.
8. S. Ludwigs, A. Bo¨ker, A. Voronov, N. Rehse, R. Magerle, G. Krausch, Nat. Mater. 2 (2003) 744-747.
9. T. J. Reece, S. Ducharme, A. V. Sorokin, M. Poulsen, Appl. Phys. Lett. 82 (2003) 142-144.
10. N. A. Kotov, I. Dekany, J. H. Fendler, J. Phys. Chem. 99 (1995) 13065-11069.
11. V. Zucolotto, K.M. Gatta's-Asfura, T. Tumolo, A. C. Perinotto, P. A. Antunes, C. J. L. Constantino, M. S. Baptista, R. M. Leblanc, O. N. Oliveira, Jr. Appl. Surf. Sci. 246 (2005) 397-402.
12. C. A. Constantine, K. M. Gatta's-Asfura, S. V. Mello, G. Crespo, V. Rastogi, T. C. Cheng, J. J. DeFrank, R. M. Leblanc, J. Phys. Chem. B 107 (2003) 13762-13764.
13. Z. Cheng, F. Su, L. Pan, M. Cao, Z. Sun Journal of Alloys and Compounds 494 (2010) L7–L10.
14. F. Henneberger, J. Puls, H. Rossmann, U. Woggon, S. Freundt, C. Spiegelberg, A. Schulzgen, J. Cryst. Growth 101 (1990) 632–642.
15. S.J. Gallagher, B. Norton, P.C. Eames, Sol. Energy 81 (2007) 813–821.
16. Y.H. Yang, M.Y. Gao, Adv. Mater. 17 (2005) 2354–2357.
17. T. Nann, P. Mulvaney, Angew. Chem. Int. Ed. 43 (2004) 5393–5396.
18. M. Darbandi, R. Thomann, T. Nann, Chem. Mater. 17 (2005) 5720–5725.
19. N.V. Hullavarad, S.S. Hullavarad, Photonic Nanostruct. 5 (2007) 156–163.
20. S.M. Reda, Acta Mater. 56 (2008) 259–264.
21. M.Q. Wang, Y.H. Xue, Z.H. Lin, X. Huo, J.P. Li, X. Yao, Mater. Lett. 62 (2008) 574–576.
22. L.E. Brus, Appl. Phys. A 53 (1991) 465–474.
23. M.M.E. Severin-Vantilt, E.W.J.L. Oomen, J. Non-Cryst. Solids 159 (1993) 38-48.
24. P. Innocenzi, M.O. Abdirashid, M. Guglielmi, J. Sol–gel Sci. Technol. 3 (1994) 47-55.
25. D. V. Talapin, A. L. Rogach, A. Kornowski, M. Haase, H. Weller, Nano Lett., 1 (2001) 207-211.
26. Y. Wei, J. Yang, J. Y. Ying, Chem. Commun. 2010, 46, 3179-3181.
27. N. Murase, C. L. Li, J. Lumin. 128 (2008) 1896-1903.
28. M. Grabolle, M. Spieles, V. Lesnyak, N. Gaponik, A. Eychmüller, U. Resch-Genger, Anal. Chem. 81 (2009) 6285-6294.
29. S. T. Selvan, T. T. Tan, J. Y. Ying, Adv. Mater. 17 (2005) 1620-1627
30. W. C. W. Chan, S. Nie, Science 281 (1998) 2016-2018.
31. D. M. Willard, L. L. Carillo, J. Jung, A. Van Orden, Nano Lett.1 (2001) 469-474.
32. F. Dubois, B. Mahler, B. Dubertret, E. Doris, C. Mioskowski, J. Am.Chem. Soc. 129 (2007) 482-483.
33. W. W. Yu, L. Qu, W. Guo, X. Peng, Chem. Mater. 15 (2003) 2854-2860
34. W. Z. Lee, G. W. Shu, J. S. Wang, J. L. Shen, C. A. Lin, W. H. Chang, R. C. Ruaan, W. C. Chou, C. H. Lu, Y. C. Lee, Nanotechnology, 16 (2005) 1517-1521.
35. A. L. Rogach, D. Nagesha, J. W. Ostrander, M. Giersig, N. A. Kotov, Chem. Mater. 12 (2000) 2676-2685.

